Re-visiting the COVID-19 analysis using the class of high ordered integer-valued time series models with harmonic features

Naushad Mamode Khan [a], Ashwinee Devi Soobhug [b,*], Noha Youssef [c], Swalay Fedally [d], Saralees Nadarajah [e], Zaid Heetun [d]

[a] *Faculty of Social Sciences and Humanities, University of Mauritius, Réduit, Mauritius*
[b] *Statistics Mauritius, Ministry of Finance, Economic Planning and Development, Port-Louis, Mauritius*
[c] *American University of Egypt, Cairo, Egypt*
[d] *Ministry of Health and Wellness, Port-Louis, Mauritius*
[e] *Department of Mathematics, University of Manchester, Manchester, United Kingdom*

ARTICLE INFO

ABSTRACT

The COVID-19 series is obviously one of the most volatile time series with lots of spikes and oscillations. The conventional integer-valued auto-regressive time series models (INAR) may be limited to account for such features in COVID-19 series such as severe over-dispersion, excess of zeros, periodicity, harmonic shapes and oscillations. This paper proposes alternative formulations of the classical INAR process by considering the class of high-ordered INAR models with harmonic innovation distributions. Interestingly, the paper further explores the bivariate extension of these high-ordered INARs. South Africa and Mauritius' COVID-19 series are re-scrutinized under the optic of these new INAR processes. Some simulation experiments are also executed to validate the new models and their estimation procedures.

1. Introduction

The Novel Coronavirus 2019 (COVID-19) pandemic had diverse repercussions on the social, cultural, economic, and psychological spheres [1]. With alarming death tolls and economic downfall, the world, especially developing countries which are more economically vulnerable, witnessed a degradation in their health system during the last two years, mainly due to emergence of variants with high propagation rate.

To exemplify, the COVID-19 pandemic affected South Africa's economy and its health care system, due to its strict sanitary restrictions like the sanitary curfew which affected hugely vulnerable households which are dependent on labour jobs. However, through rapid vaccine roll-outs and pharmaceutical interventions [2,3], a considerable decline in the number of COVID-19 infection and deaths cases, has been observed. Similar case has been observed in the Mauritian community. Mauritius, via appropriate timely health-related policies like strict COVID-19 restrictions resulting in a computational high COVID-19 stringency index was exceptionally able to curb the pandemic successfully in 2020 [See [4–6]]. After the 2021 and 2022 waves, the aim of the Mauritian authorities is now to attain herd immunity via an accelerated vaccination campaigns among high-risk patients and the whole population.

Considering that South Africa and Mauritius are Sub-Saharan countries featuring in the Top 10 most competitive economies, it is believed that by studying their COVID-19 deaths series which gives an indication of the severity of the COVID-19 pandemic, better public health strategies to strengthen the health care system and secure the lives of the South African and Mauritians, can be implemented.

When observing the COVID-19 death series in South Africa, we notice huge fluctuations with a number of ups and downs causing oscillations and with repeated trend causing periodicity. On the other hand, the COVID-19 death series in Mauritius exhibit huge variability over the mean, thus causing severe over-dispersion due to the preponderance of zeros in the early stage of detection. Besides, these series are unarguably affected by several factors which may be explaining these variations in the data such as the COVID-19 stringency index, number of COVID-19 infected people and amongst others. In addition, the COVID-19 series exhibit many significant auto-correlation lags, thus demanding a time series process of order greater than one, that is, a high-ordered process. The question of interest is how to model such series in the presence of the phenomena of periodicity, over-dispersion, presence of excess zeros, covariate specifications and others. Up to this extent, there exists integer-valued time series models of auto-regressive nature that handles the modelling of counting time series. However, these auto-regressive models are restricted as they cannot

accommodate for the above features in an unified framework. Thus, this paper proposes a flexible high-ordered integer-valued auto-regressive time series process that has the ability to simultaneously consider periodicity via harmonic specification and all sources of over-dispersion through the proper specification of the components of the time series model. The proposed model construction is a major extension of the existing models that we explain in the following subsections:

1.1. INteger-valued time series model

In the literature, integer-valued time series of auto-regressive characteristics is much popular. [7–11] propounded the class of integer-valued auto-regressive structures (INAR) based on the binomial thinning operator with constant probability coefficient [12]. The simple ordered INAR model (INAR(1)) is represented as:

$$Y_t = \rho * Y_{t-1} + R_t, t > 1, t \in \mathbb{Z} \tag{1}$$

with $\rho \in (0, 1)$, $*$ as the binomial thinning operator, and Y_t as the count observation at the tth time point. R_t is the discrete innovation term that adjusts for any possible random error effects. The binomial thinning equation is shown later in the paper, while the basic assumptions are the sequence of $\{R_t\}_{t=1}^T$ consists of independent and identically distributed innovation terms that follow some probability distributions with finite moments. The relation between the previous lagged observation Y_{-1} and the current error term R_t is such that the covariance between these two terms equates to zero. The probability generating function (PGF) of $Y_t|Y_{t-1}$ is denoted by $G_{Y_t|Y_{t-1}}(s)$ and is given by

$$G_{Y_t|Y_{t-1}}(s) = (1 - \rho + \rho s)^{Y_{t-1}} \times G_{R_t}(s) \tag{2}$$

where $G_{Y_t}(s)$ stands for the probability generating function of the random variable Y. It is worth to mention that in the development stages of the simple INAR process, the Poisson, Geometric, Negative Binomial and Poisson–Lindley innovations have been mostly used [13–17]. The choice of the innovation distributions impacts on the modelling of the over-dispersion property in the counting series Y_t. Other alternatives of the simple INAR process have been provided with random coefficient in the thinning part and with other distributed thinning distributions [18–22] to cater for the over-dispersion but the PGFs under these other thinning procedures become cumbersome. This in turn affects the estimation and inferential procedures. This paper rather focuses on the simple binomial thinning with constant coefficient.

1.2. Periodicity in the integer-valued time series process

Some examples of integer valued series with periodic structure can include the monthly counts of claims of short-term disability benefits [23,24], the day-time and night-time road accidents [25–27], the number of infected cases due to the outbreak of a virus [28,29] and, the monthly number of short-term unemployed people [30].

For such periodic series, [31] introduced the periodic integer-valued auto-regressive moving average model (PINARMA) which has the same INARMA structure in [7,8]. That is, the current observation is related with the previous-lagged observations through the binomial thinning operator [12]. If we focus on the auto-regressive structure, the PINAR model of [31] in the sense of Gladyshev [32] with period.

Basically, the PINARMA can suitably account for the non-stationarity with respect to the moments of the counting series. This is explained in detail in [31,33,34]. In our context, the model we consider is based on the INAR part of the PINARMA model involving the use of the operator of [12] and hence can generalize the stationary integer autoregressive process ($INAR$) to periodically correlated counting series, where a periodically correlated Integer-Valued process $\{Y_t, t \in \mathbb{Z}\}$ in the sense of Gladyshev (1963), with period S (where $S \geq 2$), is expressed as

$$Y_t = \rho_{1,t} * Y_{t-1} + \cdots + \rho_{p,t} * Y_{t-p} + R_t, \ t \in \mathbb{Z} \tag{3}$$

where $\{R_t, \ t \in \mathbb{Z}\}$ is a sequence of uncorrelated non-negative integer-valued random variables, with a periodic mean $\lambda_{R_t,t}$ and a finite periodic variance $\sigma^2_{R_t,t}$, and where the parameters $\rho_{i,t}$ lie in the interval $(0, 1)$ and $\theta_{j,t}$ are defined for $i = 1, \ldots, p$ and $j = 1, \ldots, q$. The mean and variance of R_t are periodic in t, with period S ($S \geq 2$), such that, $\rho_{i,t+rS} = \rho_{i,t}$, $\lambda_{R_t,t+rS} = \lambda_{R_t,t}$ and $\sigma^2_{R_t,t+rS} = \sigma^2_{R_t,t}$, $\forall t, r \in \mathbb{Z}$. The counting sequences of independent non-negative integer-valued random variables $\{Y_{k,t}, \ l \in \mathbb{N}, \ t \in \mathbb{Z}\}$, where $P(Y_{k,t} = 1) = 1 - P(Y_{k,t} = 0) = \rho_{i,t} \in [0, 1]$ is given by

$$\rho_{i,t} * Y_{t-i} = \begin{cases} \sum_{k=1}^{Y_{t-i}} b(\rho_{i,t}), & \text{if } Y_{t-i} > 0, \\ 0, & \text{if } Y_{t-i} = 0, \end{cases}$$

where $b(\rho_{i,t})$ is the Bernoulli random variable with probability $\rho_{i,t}$ ($0 < \rho_{i,t} \leq 1$). The same definition of $*$ applies to Eq. (1). From Du and Li [35], the Bernoulli sequences in the paired terms in $Y_{t,i}$ that is $(\rho_{i,t} * Y_{t-i}, \rho_{i',t} * Y_{t-i'})$ is treated independent.

Until now, the periodic INAR in Eq. (3) has been mostly used in the literature but is subject to some drawbacks. In fact, under such a parametrization, the number of model parameters increases amply as the $\rho_{i,t}$s are time-variant. This impacts on the computational procedures of the likelihood function.

2. Proposed novelties

Taking into consideration the complications involved in the estimation and computational procedures in the above existing periodic INAR process, we propose a more straightforward high-ordered INAR process based on the simple binomial thinning procedure with constant coefficient and where the error or innovation term is the random component that accounts for the periodicity by allowing its predictor function to incorporate harmonic expression of the form

$$A \sin(2\pi\omega t) + B \cos(2\pi\omega t) \tag{4}$$

where $\omega > 0$. At the same time, the underlying error distribution can consider any discrete probability model with their zero-inflated associate to handle any form of over-dispersion in the data. Under these assumptions, it is expected that the proposed high ordered INAR process is workable even though its conditional likelihood function may involve integrals. In fact, as [13] argued that with changed thinning mechanism such as the random or generalized binomial thinning, the computational performance of the conditional likelihood function is perturbed. This paper clearly aims at developing high ordered INAR model with simple constant binomial thinning under common innovation distributions with the harmonic structure that depend on the nature of the data. In the event the series is over-dispersed, the Poisson–Gamma mixture or the marginal Negative Binomial (NB) is considered since it proven lately in [36] that for over-dispersed counts, the NB yields lower fitting criterion like the Akaike Information criterion. This also implies if the series consist of huge number of zeros, we may consider the zero inflated Poisson or Negative Binomial.

Note that Eq. (4) is analogous to the definition of periodicity in the *ptest* package in R, with ω as the periodic constant. In addition, this paper proposes a bivariate INAR model with periodic structure as specified in Eq. (4) which so far has not been explored. The bivariate INAR model consists of two INAR processes wherein the two structures are inter-related by some defined mechanisms. Likewise, in [25], the cross correlation between the series was induced by the correlated innovations but we notice that this condition introduces extra parameter to estimate as we require the specification of a bivariate distribution. In this paper, we introduce in Section 5 a new bivariate INAR process where the second series is allowed to depend on the previous lag of the first series and without any dependence on the two innovation series.

The organization of the paper is as follows: In Section 3 describes the model specification, Section 4 summaries some simulation results,

Section 5 shows the findings after application of the most suitable models on the COVID-19 new deaths series in South Africa and Mauritius as well as some forecasting results. Section 5 also proposes to extend the periodic INAR to a periodic bivariate INAR model for the COVID-19 analysis. Section 6 finally summaries the important results of this research.

3. Proposed High-order INteger-valued model

By extending the simple INAR(1) process [8]) in Eq. (1) to order p, we obtain the INAR(p) process as described in [11,35]:

$$Y_t = \rho_1 * Y_{t-1} + \rho_2 * Y_{t-2} + \cdots + \rho_p * Y_{t-p} + R_t, \tag{5}$$

with $\rho_. \in (0,1)$ and $*$ as the binomial thinning operator. The same assumption of [35] holds between the lagged terms but the error or innovation term R_t is now defined with its link predictor as a function of Eq. (4), that is, $A \sin(2\pi\omega t) + B \cos(2\pi\omega t)$. Note from the Lemma 2.1 in [35], the $\sum_{j=1}^{p} \rho_j < 1$,

$$E\{(\rho_j * Y_{t-j})(\rho_{j'} * Y_{t-j'})\} = \rho_j \rho_{j'} E(Y_{t-j} Y_{t-j'}),$$

and hence,

$$Cov(\rho_j * Y_{t-j}, \rho_{j'} * Y_{t-j'}) = \rho_j \rho_{j'} Cov(Y_{t-j}, Y_{t-j'}).$$

Under the binomial thinning assumption,

$$\rho * Y_t \mid Y_t \sim Bin(Y_t, \rho)$$

$$E(Y_t) = \sum_{k=1}^{p} \rho_k E(Y_{t-k}) + E(R_t)$$

where $E(R_t) = \mu_t$ and,

$$Var(Y_t) = E(Y_t) + \sum_{k=1}^{p} \rho_k^2 [Var(Y_{t-k}) - E(Y_{t-k})] + $$
$$2 \sum_{k=1}^{p} \sum_{k<k'}^{p} \rho_k \rho_{k'} Cov(Y_{t-k}, Y_{t-k'}) + [Var(R_t) - E(R_t)]$$

Using the above, we compute the Fisher index of dispersion ($FI_{t,B}$) as a means to measure the level of over-dispersion in the INAR process of order p at time t, is given by:

$$FI_{t,B} = \frac{Var(Y_t)}{E(Y_t)} = 1 + $$

$$\left[\frac{\sum_{k=1}^{p} \rho_k^2 [Var(Y_{t-k}) - E(Y_{t-k})] + 2 \sum_{k=1}^{p} \sum_{k<k'}^{p} \rho_k \rho_{k'} Cov(Y_{t-k}, Y_{t-k'}) + [Var(R_t) - E(R_t)]}{E(Y_t)} \right]$$

Thus, for $\forall$ k $\in$ {1,p}, given $FI_{t-k,B} > 1$ and positive covariances, then $FI_t > 1$, iff, R_t is equi- or over-dispersed.

Let $\mathcal{F}_t = \{Y_{t-1}, \dots, Y_{t-p}\}$, then, the PGF in Eq. (2) is extended to

$$G_{Y_t \mid F_t}(s) = \prod_{k=1}^{p} (1 - \rho_k + \rho_k s)^{Y_{t-k}} \times G_{R_t}(s).$$

The density function $f_{y_t}(Y_t)$ is simply obtained as:

$$f_{y_t}(Y_t) = F_{y_t}(Y_t) - F_{y_t}(Y_{t-1}). \tag{6}$$

where from [37],

$$F_{y_t}(Y_t) = \frac{1}{2} - \frac{1}{2\pi} \int_{-\pi}^{\pi} Re \left[\frac{G_{y_t \mid F_t}(e^{is}, \rho_k) e^{-isY_t}}{1 - e^{-is}} \right] \tag{7}$$

and hence the log-likelihood equation is obtained as

$$\ell(\theta) = \log(\prod_{t=1}^{T} f_{y_t}(Y_t)) \tag{8}$$

where θ is the vector of the model parameters. Basically, θ consists of the regression effects such as the contributory effects of the different explanatory variables, the mean, covariance and dispersion parameters. In Section 5, the different parameters defining the vector θ are stated.
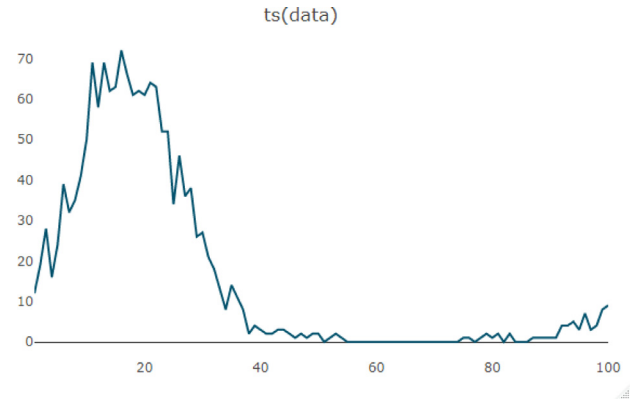

Fig. 1. Simulated data with $T = 100, \omega = 0.01$.

The log-likelihood is optimized using the *optim* function in R. From Bu et al. [38],Pedeli et al. [39],Lu [40], the vector of the estimated model parameters denoted by $(\hat{\theta})$ and the asymptotic properties of $\hat{\theta}$-$\theta \sim N(0, I^{-1}(\theta))$ where $I(\theta)$ is the Hessian, is obtained from the *optim$hessian* in R.

The reader can refer to [13,35,38,41] for more properties in the INAR(p) process. The estimation of the model parameters is handled by the Conditional maximum likelihood approach, based on the likelihood generated from the probability generating function principle explained in [37]. The R codes can be made available on request from the reader.

4. Simulation

From Section 4, we now consider an INAR(4) process with Poisson innovations as:

$$Y_t = \rho_1 * Y_{t-1} + \rho_2 * Y_{t-2} + \rho_3 * Y_{t-3} + \rho_4 * Y_{t-4} + R_t$$

where the $R_t \sim$ Poisson(λ_t) with $\lambda_t = \exp(2 \sin 2\pi\omega t + 3 \cos 2\pi\omega t)$, with $\omega > 0$. Let assume $\rho_1 = 0.2, \rho_2 = 0.1, \rho_3 = 0.1, \rho_4 = 0.05$ and $\omega = 0.01, 1.25, 3.50$. Using these values, we simulate 100, 500 and 1000 observations. The graphs and properties of these time series are shown below:

1. $T = 100$ Using the *set.seed(1234)*, the data summary for $\omega = 0.01$ gives a minimum value of 0 and a maximum of 72 with the mean and variance at 15.7 and 502.6. The data also consists of around 30% of zeros. The *ptestg* gives a *p*-value of less than 0.0001 and hence confirms the harmonic or periodic nature of the generated time series. Now with $\omega = 1.25$ and *set.seed(1235)*, we obtain the minimum value of 1 and maximum of 51, with no zero observations and has mean at 14.4 and variance 151.4. The periodicity test gives significant *p*-values. For $\omega = 3.50$ and *set.seed(1236)*, the minimum is 1 and maximum at 18 with mean 6.76 and variance 16.49 and significant periodic test. The time series plots are:

2. $T = 500$ We repeat the same experiments with same values of the thinning coefficients and ω and stored in *set.seed(2234)*, *set.seed(2235)* and *set.seed(2236)*.

In the above simulated data at $T = 500$, the mean and variance at $\omega = 0.01$ are 14.6 and 450.4 while for $\omega = 1.25$, the moment values are at 12.4 and 69.4 and at $\omega = 3.50$, they are 6.72 and 17.8. The periodic tests are all significant. It is noticeable that for the different combination of ω, the data are over-dispersed, and as ω increases, the level of periodicity also increases. For small ω, the Fisher-index of dispersion becomes more larger.

Using the above values for $\rho_.$ and ω, we generate the periodic series assuming the following three scenarios of R_t since the specifications on the assumed R_t are suitable to capture the periodicity features as shown in Figs. 1 to 6 in Section 3.
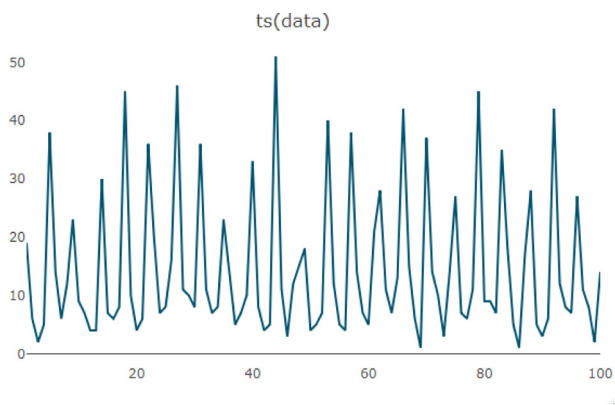
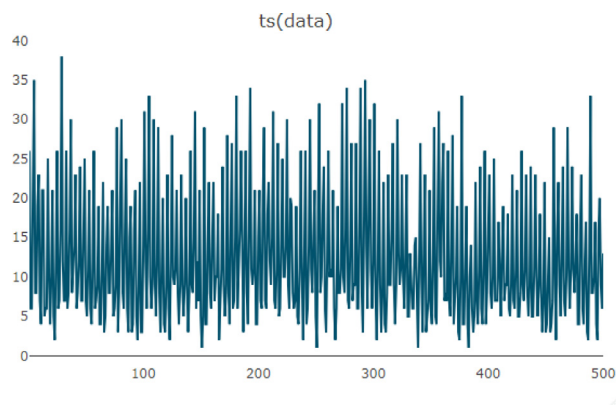**Fig. 2.** Simulated data with $T = 100, \omega = 1.25$s.

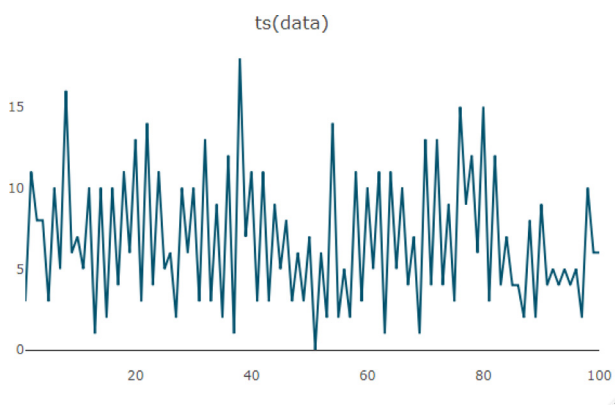**Fig. 5.** Simulated data with $T = 500, \omega = 1.25$.

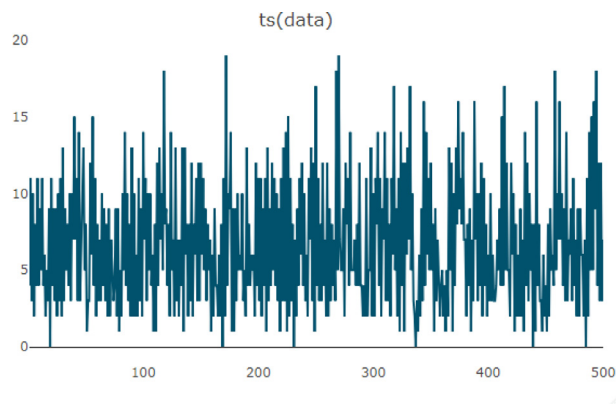**Fig. 3.** Simulated data with $T = 100, \omega = 3.50$.

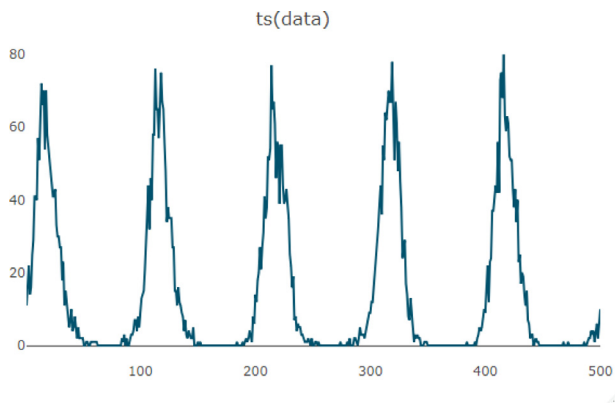**Fig. 6.** Simulated data with $T = 500, \omega = 3.50$.

Fig. 4. Simulated data with $T = 500, \omega = 0.01$.

is given by $G_{R(t)}(s) = (1 - \pi) + \left[\pi \times \exp(\lambda_t(s - 1))\right]$, where the π indicates the proportion of zeros and let $\pi = \frac{\exp(\eta)}{1 + \exp(\eta)}$.

3. R_t is Hurdle-Poisson with $\pi = 0.4$. Here we refer to the *iZID* package using the *sample.h* function. The $G_{R(t)}(s) = (1 - \pi) + \pi \times \left[\pi \times \frac{\exp(\lambda_t(s-1))}{\exp(\lambda_t)-1}\right]$

In cases 2 and 3, η is thus computed as -0.4055. The simulation results based on 500 replications are tabulated below:

Below, the boxplot representing the simulated mean estimates under Poisson innovation is given in Fig. 7:

The boxplot with the simulated mean estimates under ZI-Poisson innovation is given as Fig. 8:

The boxplot with the simulated mean estimates under Hurdle-Poisson innovation is given as Fig. 9

From the simulated results in Tables 1–3, it can be concluded that the simulated mean estimates of the model parameters on the 500 replications, in particular for the ρ and η are consistent with their corresponding population parameters. In fact, by comparing the biases, we note that the periodic INAR(4) with ZIP innovation distribution model provides estimates with lower standard errors than the other competitive INAR(4) under stationary scenario. In fact, as the number of time points increases, the standard errors of the estimates decrease thus we can say that the consistency is unaffected by the ω. Also, computationally, simulations at $T = 500$ and $T = 1000$ are very time consuming. We also attempt higher order INAR with $p > 4$ and notice that the computational procedures become very slow and time consuming.

Moreover, since the paper focused on COVID-19 analysis in countries like Mauritius, where there was a preponderance of zero COVID-19 infected and death cases in the early detection, we then consider the zero-inflated and hurdle Poisson versions in the simulations as these can mimic the actual trend of the COVID-19 in countries like Mauritius to a large extent :

1. R_t is Poisson with mean λ_t
2. R_t is Zero inflated Poisson (ZIP) with mean λ_t and with the proportion of zeros $\pi = 0.4$. In this case, we use the *ZIM* package to obtain simulated zero-inflated Poisson data using the built in function *rzip*. For the ZIP, we assume that the PGF of the ZIP
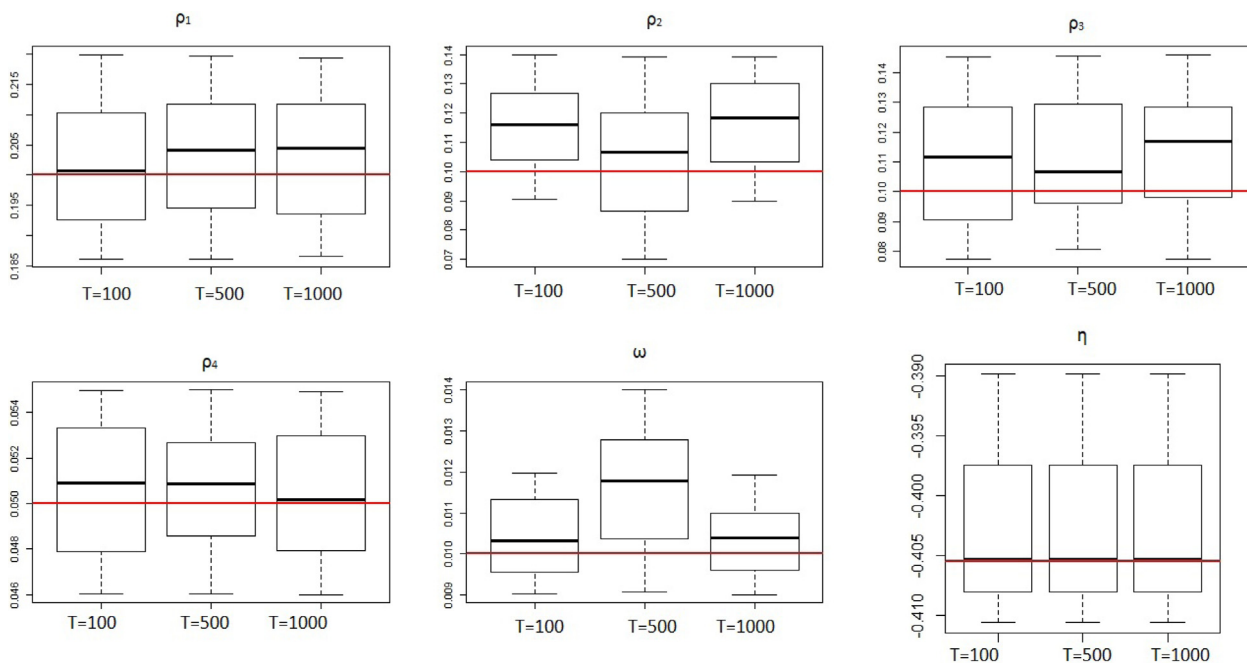
Fig. 7. Boxplot for simulated Poisson innovation with $T = 100, \omega = 0.01$.
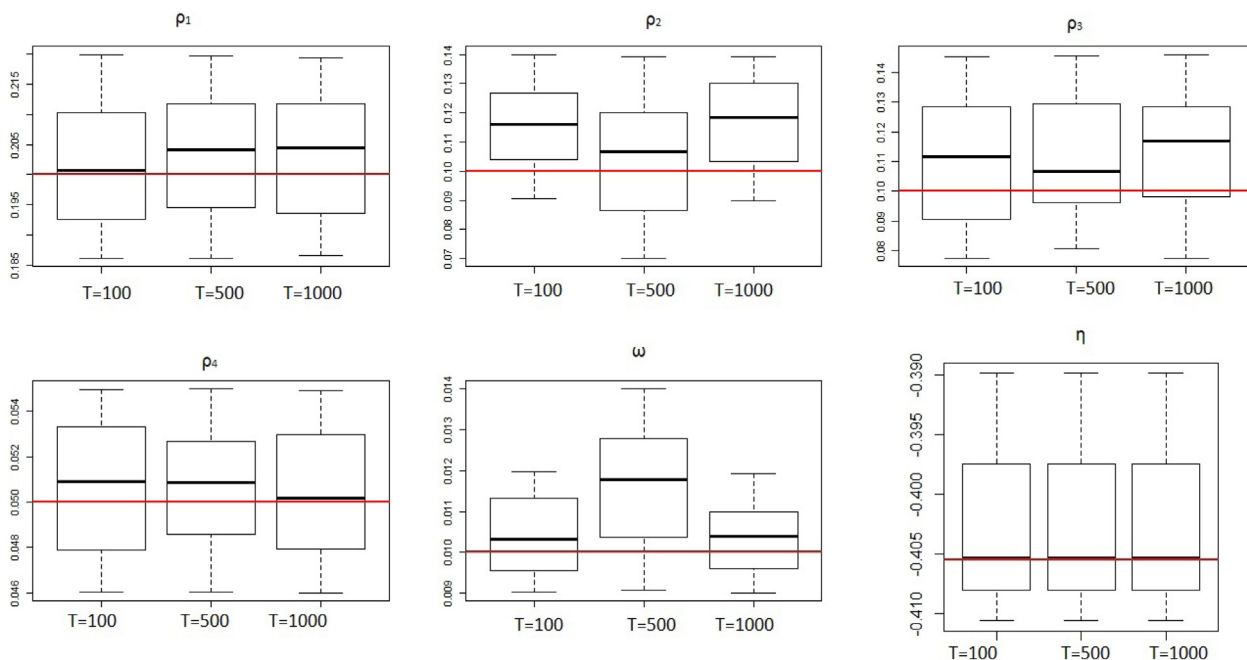
Fig. 8. Boxplot for simulated ZI-Poisson innovation with $T = 500, \omega = 1.25$.

5. Data analysis

5.1. The COVID-19 in South Africa

The plot below of the COVID-19 deaths in South Africa demonstrates three main oscillations (see Fig. 10):

The periodic test in R is also highly significant and this entails a number of significant lags. The sample mean and variance are computed as 147.8 and 23219.9 respectively and hence the high-ordered INAR model in Section 3 represents a relevant choice to analyse the COVID-19 death series in South Africa. Below, the autocorrelation (ACF) and partial autocorrelation (PACF) plots have been displayed. They clearly illustrate the existence of serial auto correlation and the number of orders (see Fig. 11):

In the presence of the above features, we fit three models to the South African COVID-19 data using the INAR(4) with Poisson innovations (Model 1), the periodic INAR (4) with Poisson innovations (Model 2) and the periodic INAR(4) with Negative Binomial innovations (Model 2 (NB)). Note that the purpose of fitting using Model 1 is to reflect on the biasedness that may occur when we ignore the

Table 1
Simulated mean estimates for $\omega = 0.01$.

Model	T	$\rho_1 = 0.2$	$\rho_2 = 0.1$	$\rho_3 = 0.1$	$\rho_4 = 0.05$	$\omega = 0.01$	$\eta = -0.4055$
Poisson	100	0.215 (0.016)	0.101 (0.015)	0.111 (0.018)	0.048 (0.009)	0.014 (0.019)	−0.3956 (0.005)
	500	0.204 (0.015)	0.095 (0.013)	0.128 (0.014)	0.053 (0.008)	0.013 (0.016)	−0.4025 (0.003)
	1000	0.189 (0.011)	0.101 (0.009)	0.146 (0.012)	0.046 (0.006)	0.009 (0.011)	−0.4061 (0.001)
ZIP	100	0.208 (0.009)	0.099 (0.006)	0.137 (0.012)	0.053 (0.009)	0.011 (0.013)	−0.4056 (0.009)
	500	0.215 (0.005)	0.145 (0.004)	0.122 (0.008)	0.05 (0.005)	0.010 (0.008)	−0.3949 (0.005)
	1000	0.186 (0.003)	0.111 (0.002)	0.105 (0.005)	0.054 (0.002)	0.012 (0.006)	−0.4022 (0.003)
HP	100	0.198 (0.005)	0.112 (0.006)	0.077 (0.010)	0.048 (0.008)	0.013 (0.009)	−0.410 (0.006)
	500	0.220 (0.003)	0.149 (0.004)	0.105 (0.009)	0.055 (0.006)	0.011 (0.008)	−0.389 (0.004)
	1000	0.218 (0.002)	0.116 (0.002)	0.142 (0.007)	0.053 (0.004)	0.014 (0.004)	−0.406 (0.003)

Table 2
Simulated mean estimates for $\omega = 1.25$.

Model	T	$\rho_1 = 0.2$	$\rho_2 = 0.1$	$\rho_3 = 0.1$	$\rho_4 = 0.05$	$\omega = 1.25$	$\eta = -0.4055$
Poisson	100	0.199 (0.021)	0.126 (0.016)	0.112 (0.019)	0.044 (0.025)	1.205 (0.011)	−0.4052 (0.006)
	500	0.214 (0.018)	0.117 (0.013)	0.106 (0.013)	0.051 (0.018)	1.196 (0.009)	−0.3998 (0.004)
	1000	0.208 (0.016)	0.089 (0.009)	0.078 (0.010)	0.049 (0.015)	1.239 (0.007)	−0.4059 (0.002)
ZIP	100	0.238 (0.019)	0.069 (0.013)	0.096 (0.012)	0.043 (0.014)	1.244 (0.019)	−0.4023 (0.009)
	500	0.201 (0.012)	0.112 (0.006)	0.099 (0.010)	0.058 (0.006)	1.231 (0.018)	−0.3965 (0.005)
	1000	0.222 (0.008)	0.126 (0.005)	0.089 (0.008)	0.051 (0.005)	1.249 (0.015)	−0.4019 (0.001)
HP	100	0.192 (0.015)	0.119 (0.011)	0.115 (0.005)	0.052 (0.008)	1.223 (0.013)	−0.4046 (0.004)
	500	0.204 (0.009)	0.122 (0.007)	0.134 (0.003)	0.046 (0.006)	1.251 (0.009)	−0.4056 (0.003)
	1000	0.239 (0.008)	0.102 (0.004)	0.144 (0.002)	0.045 (0.005)	1.196 (0.008)	−0.4002 (0.001)

Table 3
Simulated mean estimates for $\omega = 3.50$.

Model	T	$\rho_1 = 0.2$	$\rho_2 = 0.1$	$\rho_3 = 0.1$	$\rho_4 = 0.05$	$\omega = 3.50$	$\eta = -0.4055$
Poisson	100	0.177 (0.015)	0.125 (0.020)	0.067 (0.026)	0.053 (0.012)	3.489 (0.019)	−0.410 (0.021)
	500	0.191 (0.011)	0.108 (0.015)	0.089 (0.022)	0.046 (0.009)	3.523 (0.017)	−0.406 (0.019)
	1000	0.224 (0.008)	0.114 (0.011)	0.123 (0.019)	0.049 (0.005)	3.489 (0.013)	−0.390 (0.015)
ZIP	100	0.207 (0.012)	0.142 (0.019)	0.107 (0.021)	0.050 (0.009)	3.556 (0.016)	−0.406 (0.017)
	500	0.176 (0.009)	0.134 (0.015)	0.131 (0.016)	0.057 (0.007)	3.516 (0.011)	−0.405 (0.013)
	1000	0.221 (0.007)	0.066 (0.008)	0.127 (0.014)	0.055 (0.006)	3.489 (0.009)	−0.403 (0.011)
HP	100	0.179 (0.019)	0.112 (0.011)	0.133 (0.008)	0.049 (0.016)	3.467 (0.012)	−0.400 (0.009)
	500	0.219 (0.012)	0.096 (0.007)	0.149 (0.006)	0.045 (0.009)	3.562 (0.009)	−0.400 (0.006)
	1000	0.237 (0.008)	0.089 (0.005)	0.106 (0.004)	0.052 (0.006)	3.502 (0.005)	−0.403 (0.004)

periodicity in the data analysis. The estimates of the parameters under these models and their standard errors and AIC are tabulated as (see Table 4):

The parameter estimates under all models are all significant with the p values less than 0.0001. Hence, the estimates confirm that the COVID-19 death series in South Africa are to be analysed using the periodic INAR(4) process. It is noticeable that when we consider the periodicity in Model 2 and Model 2 (NB), their Akaike information criteria (AIC) have decreased and hence these two models are suitable to yield better fits. This it is important to consider the harmonic specification in the definition of the link predictor function λ_t.

Table 4
Estimates of the model parameters under both INAR (4) processes: South Africa.

Models	Parameters	ρ_1	ρ_2	ρ_3	ρ_4	λ	ω	AIC
Model 1	Estimates	0.4261	0.1698	0.1936	0.0303	0.4389		14523
	StdError	0.0002	0.0002	0.0002	0.0003	0.0004		
Model 2	Estimates	0.2632	0.2267	0.2135	0.0836		0.0158	14503
	StdError	0.0001	0.0001	0.0001	0.0002		0.0001	
Model 2 (NB)	Estimates	0.4553	0.2105	0.2241	0.0824		0.0147	14489
	StdError	0.0001	0.0001	0.0001	0.0001		0.0000	
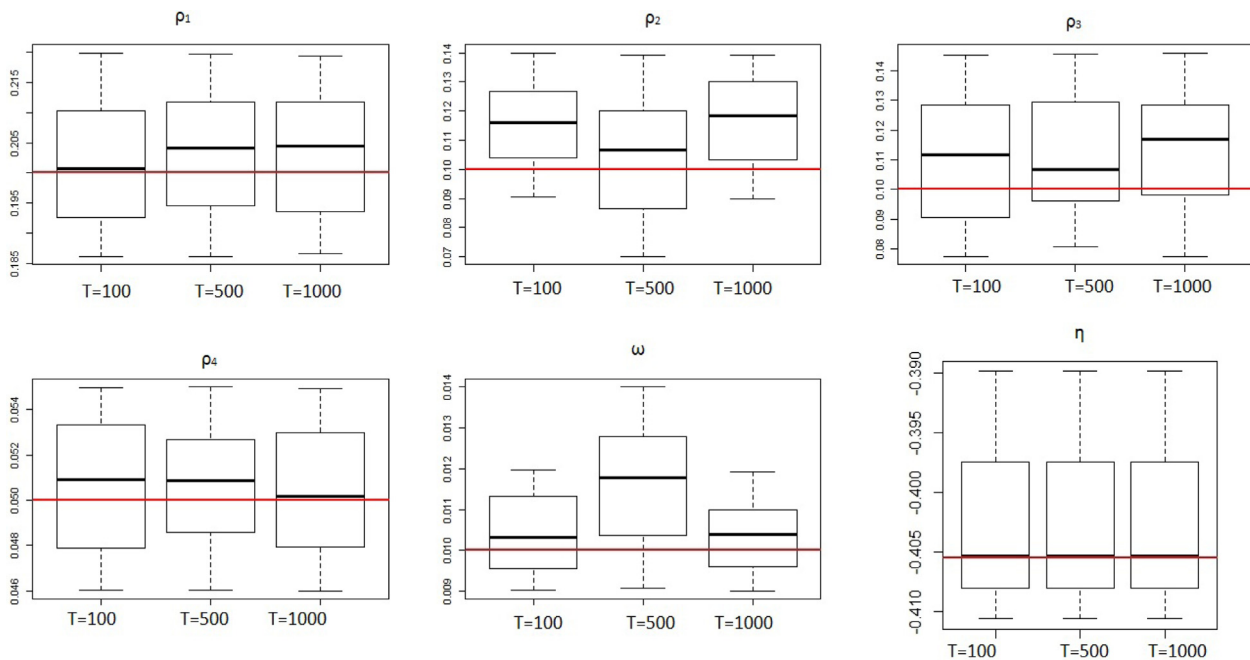
Fig. 9. Boxplot for simulated Hurdle-Poisson innovation with $T = 1000, \omega = 3.50$.
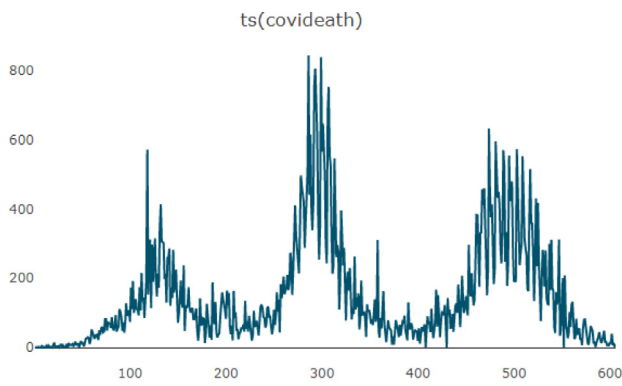
Fig. 10. COVID-19 deaths in South Africa from 27.03.2020 to 22.11.2021.

In addition, we consider the effects of some influential time-varying factors on the COVID-19 deaths such as the COVID-19 stringency index and the number of COVID-19 infected cases. The λ_t is then re-formulated as

$$\lambda_t = \exp(\beta_0 \sin 2\pi\omega t + \beta_1 \cos 2\pi\omega t) \times \text{infected}^{\beta_2} \times \text{stringency}^{\beta_3} \quad (9)$$

The COVID-19 stringency index has been computed based on nine metrics, namely school closures; workplace closures; cancellation of public events; restrictions on public gatherings; closures of public transport; stay-at-home requirements; public information campaigns; restrictions on internal movements; and international travel controls. This index

gives an indication of the strictness of the sanitary restrictions imposed in relation to the COVID-19 pandemic and the higher the value of the index, the stricter are the mentioned sanitary measures.

Refer to Table 5, Models 1 and 2 yield reliable estimates of the different parameters at very low standard errors and hence with significant p-values. However, Model 2 (NB) gives better AIC, which confirms that the periodicity in such series has to be accounted. Based on the highly significant estimates of the COVID-19 stringency index, it can be deduced that indeed the implementation of sanitary measures in South Africa like stringent lockdown, limited mobility and gatherings and legislation such as the Disaster Management Act as part of its preparedness plan, allowed South African authorities to timely detect variants and come up with proper remedial actions to strengthen the health system. This ultimately helped in reducing the COVID-19 new infection cases.

5.2. COVID-19 deaths in Mauritius

We now fit similar models to the Mauritius COVID-19 death series from 21.03.2020 to 25.04.2021 using the same influential factors as in Eq. (9). The time series plot in Figs. 12 and 13 indicates two oscillations which confirms the usage of the high ordered INAR(4) with harmonic features and even depicts over-dispersion via the *qcc.overdispersion.test* from the package *qcc*. The mean and variance of COVID-19 death series in Mauritius is around 0.03 and 0.08, respectively.

A periodic test *p*-value of 0.0285 from the *ptestg* function in the package *ptest* in R, was obtained. The application results are (see Table 6):

Table 5

Estimates of the model parameters under both INAR(4) with covariates: South Africa.

Models	Parameters	ρ_1	ρ_2	ρ_3	ρ_4	β_0	β_1	β_2	β_3	ω	AIC
Model 1	Estimates	0.4588	0.1704	0.1784	0.0202			0.0086	0.0078		14352
	StdError	0.0001	0.0001	0.0004	0.0024			0.0002	0.0003		
Model 2	Estimates	0.4527	0.1557	0.1839	0.0295	0.0081	0.0059	0.0151	0.0059	0.0113	14246
	StdError	0.0002	0.0002	0.0003	0.0003	0.0032	0.0002	0.0002	0.0003	0.0002	
Model 2 (NB)	Estimates	0.4426	0.1601	0.1855	0.0249	0.0083	0.0057	0.0147	0.0048	0.0109	14219
	StdError	0.0001	0.0002	0.0001	0.0002	0.0024	0.0002	0.0002	0.0004	0.0002	

Table 6

Estimates of the INAR(4): COVID-19 Mauritius death series.

Models	Parameters	ρ_1	ρ_2	ρ_3	ρ_4	β_0	β_1	β_2	β_3	ω	AIC
Model 1	Estimates	0.2125	0.1071	0.1071	0.0537			0.0107	0.0079		25030
	StdError	0.0036	0.0063	0.0089	0.0051			0.0042	0.0069		
Model 2	Estimates	0.1421	0.0925	0.1067	0.0572	0.0145	0.0123	0.0132	0.0151	0.0042	25024
	StdError	0.0117	0.0192	0.0099	0.0128	0.0033	0.0056	0.0046	0.0031	0.0126	
Model 2 (NB)	Estimates	0.1650	0.0856	0.1029	0.0500	0.0092	0.0107	0.0104	0.0111	0.0116	20080
	StdError	0.0100	0.0071	0.0062	0.00678	0.0063	0.0035	0.0032	0.0028	0.0087	

Table 7

Estimates of Parameters of INAR(4) with ZI and HP Poisson and Negative Binomial innovations: Mauritius COVID-19 Death series.

Models	Parameters	ρ_1	ρ_2	ρ_3	ρ_4	β_0	β_1	β_2	β_3	ω	η	AIC
Model 1	Estimates	0.1438	0.1119	0.1085	0.0524			0.0114	0.0115		0.9212	25025
	StdError	0.0051	0.0095	0.0099	0.0071			0.0025	0.0021		0.0041	
Model 2 (ZIP)	Estimates	0.1414	0.1111	0.1064	0.0513	0.0109	0.0109	0.0107	0.0116	0.0105	0.9310	25019
	StdError	0.0094	0.0062	0.0041	0.0055	0.0034	0.0028	0.0024	0.0037	0.0023	0.0027	
Model 2 (ZINB)	Estimates	0.1754	0.0981	0.0907	0.0492	0.0112	0.0113	0.0084	0.0092	0.0105	0.9112	20078
	StdError	0.0071	0.0054	0.0034	0.0042	0.0026	0.0033	0.0022	0.0032	0.0021	0.0023	
Model 3 (HP)	Estimates	0.1456	0.1122	0.1054	0.0523	0.0109	0.011	0.0111	0.0121	0.0107	0.0105	25020
	StdError	0.0095	0.0065	0.0041	0.0052	0.0036	0.0031	0.0022	0.0032	0.0021	0.0027	
Model 3 (HNB)	Estimates	0.1456	0.1122	0.1054	0.0523	0.0109	0.011	0.0111	0.0121	0.0107	0.0105	21010
	StdError	0.0095	0.0065	0.0041	0.0052	0.0036	0.0031	0.0022	0.0032	0.0021	0.0027	

From the above results, it is clear that the Model 2 (NB) gives better AIC. The over-dispersion parameter is estimated at 0.4282 with sd 0.0362. Overall, all models yield significant estimates with low *p*-values. Furthermore, since the series contain an excess of zeros amounted to 97.3% as compared to the South African COVID-19 data, we may choose to re-run the periodic INAR model with the zero-inflated Poisson (ZIP) and zero-inflated Negative-Binomial innovations (Model 2: ZINB) or the Hurdle Poisson innovation (Model 3: HP) and Hurdle Negative-Binomial (Model 3:HNB). The results are shown in Table 7:

The Model 1 is the INAR(4) with ZI Poisson innovations without any periodicity feature. The Model 2 (ZINB) outperforms the others with an over-dispersion estimated at 0.4281 and with standard errors at 0.0023, which implies that such COVID series can better be modelled using the periodic INAR with NB innovations. Timely imposition of new immediate sanitary measures during the peak COVID-19 phases like sanitary curfew/lockdown, sanitization and sensitization campaigns and safe shopping guidelines, allowed Mauritius in 2020, to be among those countries which have curbed the COVID-19 pandemic, in a record time. At that time, COVID-19 stringency index was on the higher side. In 2021/2022, by re-enforcing the COVID-19 related laws like mandatory vaccination with booster dose and wearing of face-masks in public places, the COVID-19 situation was under controlled.

5.3. Forecasts

The forecasts for Mauritius and South Africa are estimated from the periodic model. For South Africa, the period from 23.11.2021 to 02.12.2021 is considered using the Model 2 results in Table 5 while for Mauritius, the forecasting period starts from 26.04.2021 to 05.05.2021 using the Model 2 (ZINB) in Table 7 since it yields the best AIC (see Fig. 14).

The forecasts reaped satisfactory RMSEs notably for South Africa which was around 5.29 whilst for Mauritius, around 1.73. Below, is the confidence interval (see Fig. 15):

5.4. Extension

We can consider an extension of the periodic INAR to a periodic bivariate INAR model of the following form for the COVID-19 analysis:

$$Y_{t,1} = \rho_{11} * Y_{t-1,1} + R_{t,1}$$
$$Y_{t,2} = \rho_{21} * Y_{t-1,2} + \rho_{22} * Y_{t-1,1} + R_{t,2}$$

where $Y_{t,1}$ measures the number of COVID-19 infected cases at the *t*th time point and $Y_{t,2}$ is the corresponding number of COVID-19 deaths, with $R_{t,1} \sim \text{NegBinom}(c, \lambda_{t,1})$, where $NegBinom$ is the Negative-Binomial (NB) distribution with size $1/c$ and mean $\lambda_{t,1}$ and $R_{t,2}$ is the Zero-inflated Poisson (ZIP) with mean $\lambda_{t,2}$ and probability of zeros denoted by π_2. The choice of the NB model for $R_{t,1}$ is because the series $Y_{t,1}$ is found to be hugely over-dispersed, while the ZIP model for $R_{t,2}$ is justified since the death series is characterized by 97.5% number of zeros. The covariance between $Y_{t,1}$ and $Y_{t,2}$ is given by

$$Cov(Y_{t,1}, Y_{t,2}) = Cov(\rho_{11} * Y_{t-1,1}, \rho_{21} * Y_{t-1,2})$$
$$+ Cov(\rho_{11} * Y_{t-1,1}, \rho_{22} * Y_{t-1,1})$$

where $Cov(R_{t,1}, R_{t,2}) = 0$. The $*$ operator is the usual binomial thinning. The assumption on the previous lagged term $Y_{t-j,k}$ and $R_{t,k}$ holds as in the classical INAR time series model. The Bernoulli sequences in the paired terms in $Y_{t,2}$ that is $(\rho_{21} * Y_{t-1,2}, \rho_{22} * Y_{t-1,1})$ is treated independent. The marginal means of $R_{t,1}$ and $R_{t,2}$ are given as:

$$\lambda_{t,1} = \exp(\beta_{10} \sin 2\pi\omega_1 t + \beta_{11} \cos 2\pi\omega_1 t) \times \times \text{stringency}^{\beta_{12}}$$
$$\lambda_{t,2} = \exp(\beta_{20} \sin 2\pi\omega_2 t + \beta_{21} \cos 2\pi\omega_2 t) \times \times \text{stringency}^{\beta_{22}}$$
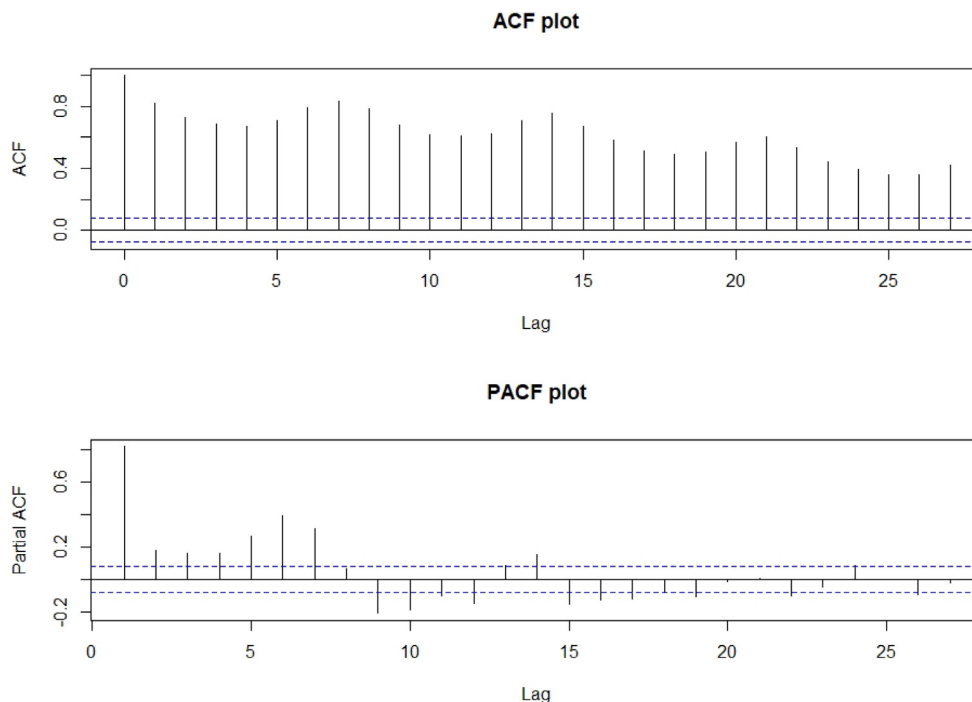
ACF plot

PACF plot

Fig. 11. ACF and PACF plots for COVID-19 deaths in South Africa.
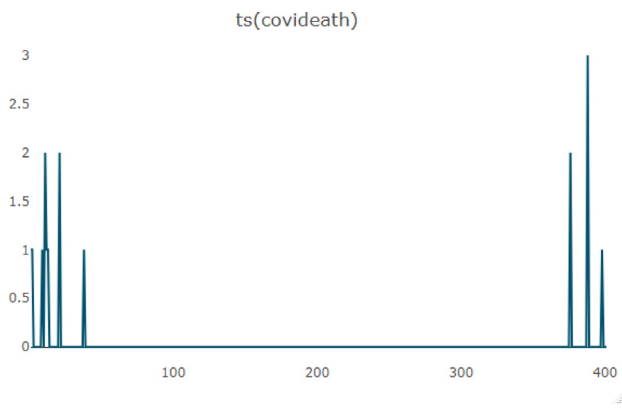
ts(covideath)

Fig. 12. COVID-19 deaths in Mauritius from 21.03.2020 to 25.04.2021.

Table 8
Estimates of the BINAR process.

Parameters	ρ_{11}	ρ_{21}	ρ_{22}	ρ_{21}	ω_1	ω_2
Estimates	0.0581	0.0582	0.0225	0.9351	0.4318	0.7805
StdError	0.0044	0.0039	0.0042	0.0076	0.0001	0.0001

Table 9
Estimates of the BINAR process.

Parameters	π_2	β_{10}	β_{11}	β_{12}	β_{20}	β_{21}	β_{22}
Estimates	0.9698	0.3172	0.1426	0.3194	0.4227	0.2226	0.2851
StdError	0.0107	0.0113	0.0105	0.0004	0.0485	0.0753	0.0251

The representations of the Negative-Binomial and Zero-inflated Poisson are given in Appendix. Since the COVID-19 series from Mauritius did not consist of huge values for both cases and deaths, we apply the proposed periodic BINAR(1) and the results are summarized in (see Tables 8 and 9):

The AIC is 1825.681 with log-likelihood value as 925.8406.

6. Conclusion

This paper brings an important finding in the class of integer-valued auto-regressive models. For series with harmonic or periodic structure, it is inevitable to consider the periodic feature with some harmonic functions in the definition of the innovation predictor function. This subsequently impacts on the significance of the explanatory variables and fitting criteria of the time series models. Whilst, the choice of the error term is determined by the level of over-dispersion in the data and the presence of zeros. Thus, the proposed INAR(p) model is quite flexible as it accommodates for all these possible features. In the presence of over-dispersion and excess zeros, we consider the Poisson and Negative-Binomial and their zero inflated associates in the error term specification. Such specification suits the pattern shown in the COVID-19 series for South Africa and Mauritius. Additionally, if the series has comfortably lower integer-values, the periodic INAR with Poisson mixture innovations is recommended. The paper explores the periodicity in the high ordered integer-valued INAR models and also extends prominently to the bivariate INAR model. Under both cases, the results are reliable and helpful to the authorities in terms of the COVID-19 stringency monitoring campaigns. The proposed periodic high ordered models with their bivariate extension can be applied to other countries' COVID-19 data with additional official information on the explanatory variables to better infer their respective influences on the COVID-19.

Declaration of competing interest

The authors declare that they have no known competing financial interests or personal relationships that could have appeared to influence the work reported in this paper.

Acknowledgements
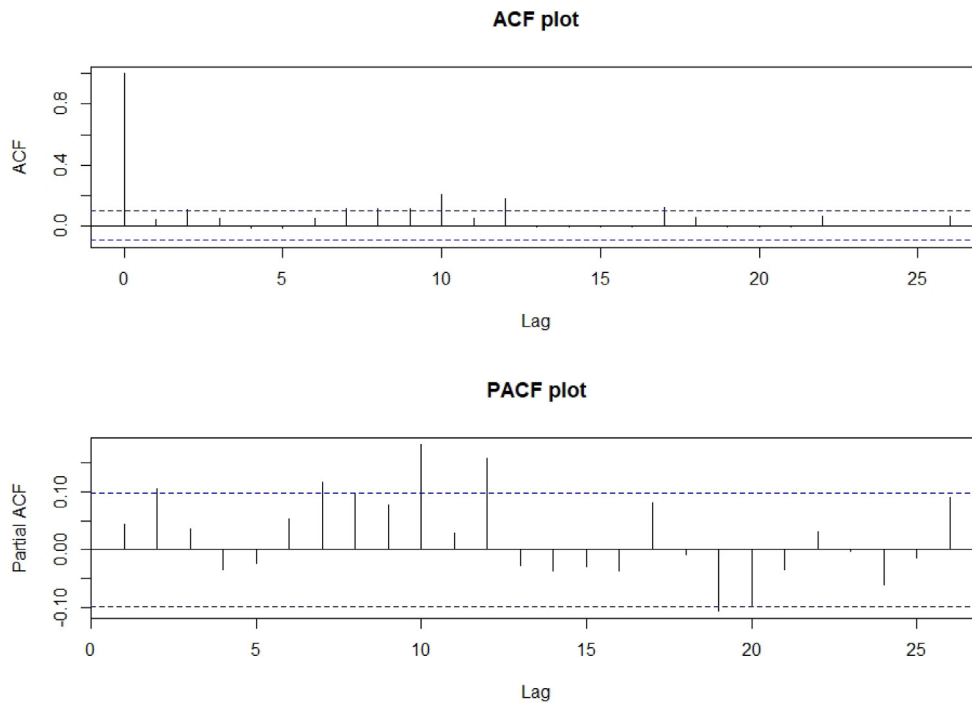
ACF plot

PACF plot

Fig. 13. ACF and PACF plots of COVID-19 deaths in Mauritius.

Forecasted of new COVID-19 deaths in South Africa

Forecasted of new COVID-19 deaths in Mauritius

Fig. 14. Forecasts for next 10 days.

Forecasted death values within 95% CI (Mauritius)

Forecasted death values within 95% CI (South Africa)
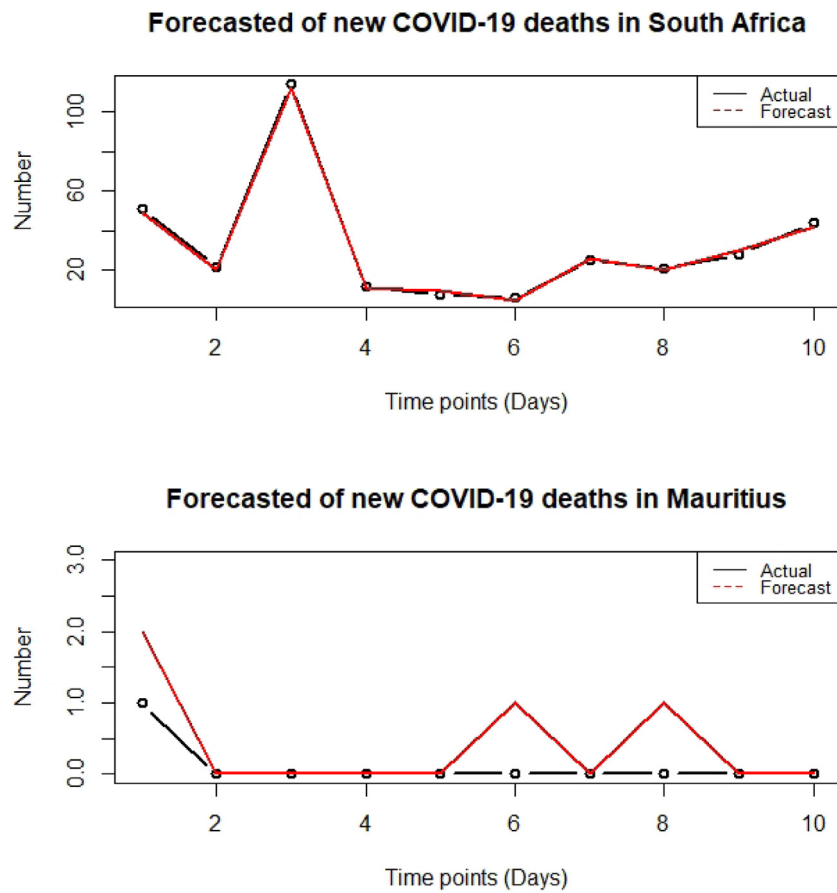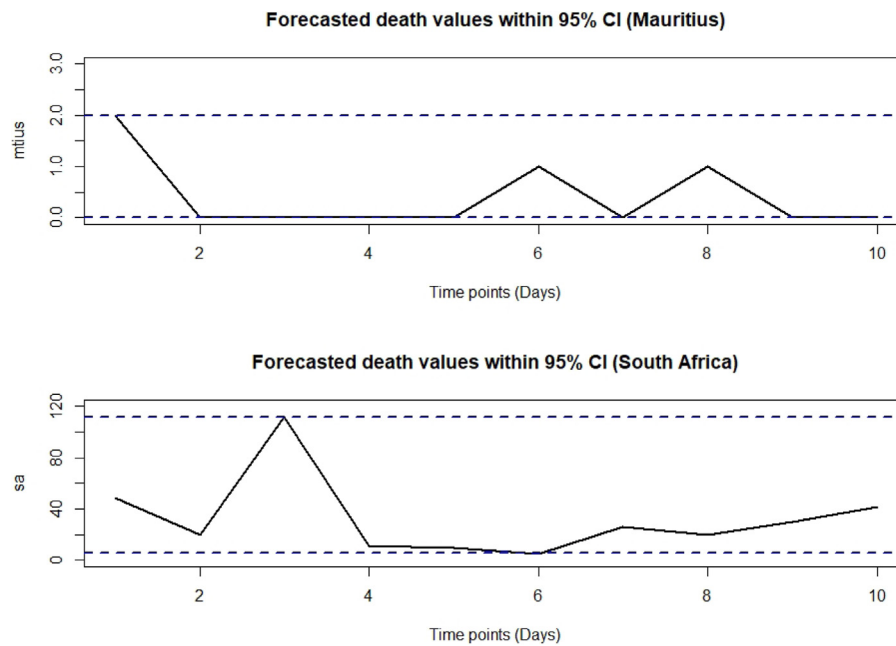
Fig. 15. The forecasts within 95% CI.

Appendix

The NB with size c and mean $\lambda_{t,1}$ is given as:

$$P(R_t = r) = \frac{\Gamma(r + c^{-1})}{\Gamma(r+1)c^{-1}!} \left[\frac{c^{-1}}{\lambda_{t,1} + c^{-1}}\right]^{c^{-1}} \left[\frac{\lambda_{t,1}}{\lambda_{t,1} + c^{-1}}\right]^r$$

and has $E(R_t) = \lambda_{t,1}$ and $V(R_t) = \lambda_{t,1}(1 + c\lambda_{t,1})$, where $c > 0$. The ZIP with parameters π_2 and $\lambda_{t,2}$ is expressed as

$$P(R_t = r) = \begin{cases} \pi_2 + (1-\pi_2)P(r=0), r = 0 \\ (1-\pi_2)\exp(-\lambda_{t,2})\frac{\lambda_{t,2}^r}{r!}, r = 1, 2, 3, \ldots \end{cases}$$

with $E(R_t) = \lambda_{t,2}(1-\pi_2)$ and $V(R_t) = \lambda_{t,2}(1-\pi_2)(1 + \lambda_{t,2}\pi_2)$ with $\lambda > 0, 0 < \pi_2 < 1$. By assessing the Fisher index of dispersion for both models, we can notice that both NB and ZIP are suited for modelling the overdispersion in the COVID-19 cases and death series.

References

[1] A. Soobhug, N. Mamode Khan, D. Gokulsing, Exploring the Consequences of the Covid-19 Pandemic: The Impacts of the Novel Coronavirus 2019 on Vulnerable Groups of Society: The Case for Mauritius, Vol. 1, Apple Academic Press, 2022.

[2] K. Linka, M. Peirlinck, E. Kuhl, The reproduction number of COVID-19 and its correlation with public health interventions, 3, 2020, pp. 1–16, medRxiv.

[3] A. Chudik, M.H. Pesaran, A. Rebucci, COVID-19 time-varying reproduction numbers worldwide: an empirical analysis of mandatory and voluntary social distancing, 2021, medRxiv.

[4] N. Mamode Khan, A. Soobhug, M. Heenaye-Mamode Khan, Studying the trend of the novel coronavirus series in Mauritius and its implications, PLoS One 15 (7) (2020).

[5] A. Soobhug, H. Jowaheer, N. Mamode Khan, N. Reetoo, K. Meethoo Badulla, L. Musango, C. Kokonendji, A. Chutoo, N. Aries, Re-analyzing the SARS-CoV-2 series using an extended integer-valued time series models: a situational assessment of the COVID-19 in mauritius, PLoS One (2022).

[6] L. Musango, L. Veerapa Mangroo, Z. Joomaye, A. Ghurbhurrun, V. Vythelingam, E. Paul, Key success factors of mauritius in the fight against COVID-19, BMJ Global Health 6 (2021).

[7] E. McKenzie, Some simple models for discrete variate time series, Water Resour. Bull. 21 (4) (1985) 645–650.

[8] E. McKenzie, Autoregressive moving-average processes with negative binomial and geometric marginal distrbutions, Adv. Appl. Probab. 18 (1986) 679–705.

[9] M. Al Osh, A. Alzaid, Integer-valued moving average (INMA) process, Statist. Papers 29 (1988) 281–300.

[10] A. Alzaid, M. Al Osh, First-order integer-valued autoregressive (INAR(1)) process: Distribution and regression properties, Stat. Neerlandica 42 (1) (1988) 53–61.

[11] A. Alzaid, M. Al Osh, An integer-valued pth order autoregressive structure (INAR(p)) process, J. Appl. Probab. 27 (1990) 314–324.

[12] F. Steutel, K. Van Harn, Discrete analogues of self-decomposability and stability, Ann. Probab. 7 (1979) 893–899.

[13] H. Joe, Likelihood inference for generalized integer autoregressive time series models, Econometrics 7 (2019) 43.

[14] C. Weiß, A Poisson INAR(1) model with serially dependent innovations, Metrika 78 (2015) 829–851.

[15] M. Mohammadpour, H. Bakouch, M. Shirozhan, Poisson–Lindley INAR(1) model with applications, Braz. J. Probab. Stat. 32 (2018) 262–280.

[16] M. Bourguignon, J. Rodrigues, M. Santos Neto, Extended Poisson INAR(1) processes with equidispersion, underdispersion and overdispersion, J. Appl. Stat. 46 (2019) 101–118.

[17] M. Bourguignon, J. Rodrigues, M. Santos Neto, Extended Poisson INAR(1) processes with equidispersion, underdispersion and overdispersion, J. Appl. Stat. 46 (2019) 101–118.

[18] C.H. Weiß, An Introduction to Discrete-VAlued Time Series, Wiley, Chichester, 2018.

[19] M. Ristic, H. Bakouch, A. Nastic, A new geometric first-order integer-valued autoregressive (NGINAR(1)) process, J. Statist. Plann. Inference 136 (2009) 2218–2226.

[20] C.H. Weiß, Thinning Operations for Modeling Time Series of Counts - A Survey, Vol. 92, Springer-Verlag, 2008, pp. 319–341.

[21] A. Nastic, H. Bakouch, A combined geometric INAR(p) model based on negative binomial thinning, Math. Comput. Modelling 55 (2012) 1665–1672.

[22] M. Scotto, C.H. Weiß, S. Gouveia, Thinning-based models in the analysis of integer-valued time series: A review, Stat. Modell. 15 (2015) 590–618.

[23] R. Freeland, Statistical Analysis of Discrete Time Series with Applications to the Analysis of Workers Compensation Claims Data, University of British Columbia, Vancouver (Canada), 1998.

[24] K. Fokianos, Count time series models, in: Time Series-Methods and Applications, Vol. 30, 2012, pp. 315–347.

[25] X. Pedeli, D. Karlis, A bivariate INAR(1) process with application, Stat. Modell.: Int. J. 11 (4) (2011) 325–349.

[26] T. Brijs, D. Karlis, G. Wets, Studying the effect of weather conditions on daily crash counts using a discrete time series model, Accid. Anal. Prev. 40 (3) (2008) 1180–1190.

[27] D. Karlis, G. Sermaidis, T. Brijs, Discrete valued time series models for examining weather effects in daily accident counts, Stat. Modell. (2008).

[28] R. Ferland, A. Latour, D. Oraichi, Integer-valued GARCH process, J. Time Series Anal. 27 (2006) 923–942.

[29] S. Chan, J. Chu, Y. Zhang, S. Nadarajah, Count regression models for COVID-19, Physica A 563 (2021) 125460.

[30] M. Monteiro, M. Scotto, I. Pereira, A periodic bivariate integer-valued autoregressive model, Mathematics (2015).

[31] M. Bentarzi, N. Aries, On some periodic inarma(p,q) models, J. Commun. Stat. - Simul. Comput. (2020).

[32] E. Gladysev, Periodically correlated random sequences, Sov. Math. 2 (1961) 385–388.

[33] P. Filho, V. Reisen, P. Bondon, M. Ispany, M.M. Melo, F. Serpa, A periodic and seasonal statistical model for non-negative integer-valued time series with an application to dispensed medications in respiratory diseases, Appl. Math. Model. 96 (2021) 545–558.

[34] M. Bentarzi, W. Bentarzi, Periodic integer-valued GARCH(1,1) model, Comm. Statist. Simulation Comput. 46 (2) (2017) 1167–1188.

[35] J. Du, Y. Li, The integer-valued autoregressive (INAR(p)) model, J. Time Series Anal. 12 (1991) 129–142.

[36] A. Chutoo, D. Karlis, N. Mamode Khan, V. Jowaheer, The unilateral spatial autoregressive process for the regular lattice two-dimensional spatial discrete data, SORT (2021).

[37] R. Davies, Numerical inversion of a characteristic function, Biometrika 60 (1973) 415–417.

[38] R. Bu, B. McCabe, K. Hadri, Maximum likelihood estimation of higher-order integer-valued autoregressive processes, J. Time Series Anal. 29 (2008) 973–994.

[39] X. Pedeli, A.C. Davison, F. Konstantinos, Likelihood estimation for the inar(p) model by saddlepoint approximation, J. Amer. Statist. Assoc. 110 (2015) 1229–1238..

[40] Y. Lu, Exact Likelihood Estimation and Probabilistic Forecasting in Higher-order INAR(p) Models, MPRA Paper 83682, University Library of Munich, Munich, 2018.

[41] N. Mamode Khan, H. Bakouch, A. Soobhug, M. Scotto, Insights on the trend of the Novel Coronavirus 2019 series in some Small Island Developing States: A Thinning-based Modelling Approach, Alexandria Eng. J. 60 (2) (2021) 2535–2550.